Acta Cryst. (1978). B**34**, 3005–3011

The Crystal Structure of the π-Molecular Complex of Anthracene with Pyromellitic Dianhydride at −120°C

By Beverly E. Robertson* and John J. Stezowski†

Institut für Organische Chemie, Biochemie und Isotopenforschung der Universität Stuttgart, Pfaffenwaldring 55, 7000 *Stuttgart* 80, *Federal Republic of Germany*

(*Received* 24 *February* 1978; *accepted* 5 *May* 1978)

An analysis of $C_{14}H_{10}.C_{10}H_2O_6$ has been made for a crystal at −120 (2)°C: a = 7·2812 (6), b = 10·7684 (7), c = 7·1246 (7) Å, α = 117·516 (7), β = 111·513 (8), γ = 97·437 (8)°, Z = 1. The refinement with the full data set (3769 observed reflections, $\sin\theta/\lambda \leq 0{\cdot}910$ Å^{-1}, λ = 0·71069 Å) converged with R = 0·046 and R_w = 0·062. A comparison of refinements with truncated data sets: $0{\cdot}478 \leq \sin\theta/\lambda \leq 0{\cdot}91$ Å^{-1} and $\sin\theta/\lambda \leq 0{\cdot}610$ Å^{-1} is presented. The crystal packing is examined in detail in an effort to determine which structural properties arise therefrom and thus not from charge-transfer effects. Comparison with crystal structures for non-complexed anthracene and pyromellitic dianhydride indicate that the low-temperature crystal structure determination has not revealed detectable changes in bonding geometry due to formation of the complex.

Introduction

The π-molecular complex between anthracene and pyromellitic dianhydride, A-PMDA, has been found to give high-quality single crystals particularly suitable for spectroscopic study. For example, Eckhardt & Merski (1973) have determined piezoreflection spectra for a crystal glued to a piezoceramic disk and Karl & Ziegler (1975) have reported photocurrent excitation spectra of A-PMDA single crystals. Interpretation of the spectral data can benefit from a knowledge of the crystal structure.

Boeyens & Herbstein (1965) have reported a structure determination for A-PMDA based on a limited room-temperature data set. In view of the considerable interest in the solid-state properties of the complex, we felt a more precise determination was needed. We have carried out such an analysis for a single crystal cooled to −120 (2)°C and are able to report that improvement in agreement between spectroscopic measurements and the crystal structure model has resulted. The orientation of the z axis of the fine-structure tensor of the lowest excited state of the A-PMDA complex determined at room temperature by Ziegler & Karl (1978) now coincides to within 1° with the normal to the plane of the central ring of the anthracene molecule, whereas substantial deviations are obtained with the data from the earlier determination. The current results are consistent with spectroscopic indications (Haarer & Karl, 1973; Keijzers & Haarer, 1977) that this excited state is essentially a pure anthracene triplet.

Experimental

Crystals of A-PMDA from two independent laboratories were examined. Our studies were initiated with crystals grown from solution in the laboratories of C. J. Eckhardt and were subsequently extended to include photographic examination of sublimation-grown crystals provided by N. Karl. All crystals examined were of the same crystalline phase and were generally similar in appearance. They were bright red, transparent, and displayed well-formed faces. Perhaps the one noteworthy difference between the solution- and sublimation-grown crystals was an apparently higher propensity for macroscopic twinning in the latter. The three crystals we examined from the sublimed samples displayed diffraction patterns indicative of some degree of such twinning on the (110) plane whereas no such indication was found in the solution-grown crystals. The presence of such twinning can be detected by examination with a polarizing microscope. The crystals were usually long flat needles which, for the untwinned examples, are characterized as follows: The needle axis is the crystallographic c axis, the larger plate faces are (010) and the smaller are $(1\bar{1}0)$ planes.

A nearly equidimensional (0·5 mm on a side) crystal, cleaved from a needle taken from the solution-grown sample was encased in a thin-walled glass capillary. All

---

* Present address: Faculty of Science, University of Regina, Regina, Saskatchewan S4S 0A2, Canada.

† Author to whom correspondence should be sent.

Table 1. *Lattice constants*

Edge lengths are in Å. Angles are in degrees.

	This work, −120 (2)°C	This work, 22°C
a	7·2812 (6)	7·37 (1)
b	10·7684 (7)	10·78 (1)
c	7·1246 (7)	7·23 (1)
α	117·516 (7)	117·5 (1)
β	111·513 (8)	111·3 (1)
γ	97·437 (8)	97·5 (1)

Molecular formula $C_{14}H_{10}.C_{10}H_2O_6$

$M_r = 396·36$

Space group $P\bar{1}$

$Z = 1$

$V = 330·40$ Å^3

$F(000) = 204$

μ(Mo $K\alpha$) = 1·20 cm^{-1}

λ(Mo $K\alpha$) = 0·71069 Å

quantitative crystallographic measurements were made with this crystal on a Syntex $P\bar{1}$ autodiffractometer equipped with a low-temperature device (Syntex LT-1). A preliminary set of lattice parameters was determined for the crystal at room temperature, from the angular coordinates of seven reflections. The final lattice parameters were obtained for the cooled crystal [−120 (2)°C] by the least-squares method* with automatically centered 2θ values of 59 reflections in the angular range $35 \leq 2\theta \leq 45°$; both sets are presented in Table 1. Intensities were measured in an ω-scan mode for which the scan rate was allowed to vary as a function of maximum peak intensity from 2·0 to 24·0° min^{-1}; a scan range of 0·75° was measured and background intensity was measured on each side of the reflection for one half the total scan time. Of the 5299 unique reflections so measured, $\sin\theta/\lambda \leq 0·91$ Å^{-1} [λ(Mo $K\alpha$) = 0·71069 Å], 3769 were classified as observed [$I \geq 3\sigma(I)$]. Three reference reflections, monitored after each 200 data were measured, displayed a systematic decrease in their intensity totalling *ca* 10%. The data were subsequently corrected for this decrease and for Lorentz and polarization effects, but not for absorption (μ = 1·20 cm^{-1}).

Structure determination and refinement

The structure was solved by direct methods and refined by a full-matrix least-squares method. Initial refinement of C and O atoms with anisotropic temperature factors and unit weights resulted in $R = 0·073$. Addition of the H atoms, for which the initial calculated coordinates and isotropic temperature factors were also refined, reduced R to 0·058. At this stage the average e.s.d. in a C—C bond was 0·004 Å. Further refinement with empirically weighted data: $w = 1/\sigma^2$, where $\sigma = \sigma(F_o) + 0·0125|F| + 0·0009|F_o|^2$ and $\sigma(F_o)$ is based on counting statistics and variations in the reference reflections, resulted in a final $R = 0·046$ and $R_w = 0·062$ for the contributing reflections.* Examination of the data demonstrated the lack of extinction. The average e.s.d. in a C—C bond was reduced to 0·0014 Å.

The high resolution of the data and the resultant favorable data to parameter ratio (23·6) afforded the opportunity to examine the effects of various limitations of the $\sin\theta/\lambda$ range in the refinement. Lemley, Skarstad & Hughes (1976) have reported the refinement of 1,1,2,2-tetracyanocyclopropane in which they found that elimination of low-angle data resulted in lengthening of the C≡N bond by an average of 0·011 Å. We felt that a similar refinement for a structure with numerous bonds for which the bond order, n, is describable as $1 \leq n \leq 2$ would be of interest. We also decided to probe the effect that truncation of the high-angle data would have on the bond distances of the refined structure. Therefore in addition to the refinement with the full set of data (REF 1) we conducted additional refinements with (*a*) data consisting of reflections for which $0·478 < \sin\theta/\lambda < 0·910$ Å^{-1}

Table 2. *Results of three refinements*

	REF 3	REF 1	REF 2
$\sin\theta/\lambda$ (max) (Å^{-1})	0·610	0·910	0·910
$\sin\theta/\lambda$ (min) (Å^{-1})	0·000	0·000	0·478
Number of reflections	1389	3769	3048
R	0·039	0·046	0·042
R_w	0·055	0·062	0·059
C(1)–C(2)	1·3894	1·3913	1·3921
C(1)–C(3')	1·3886	1·3898	1·3905
C(2)–C(3)	1·3959	1·3986	1·3984
C(2)–C(4)	1·4897	1·4854	1·4861
C(3)–C(5)	1·4856	1·4834	1·4845
C(9)–C(10)	1·3996	1·4014	1·4038
C(9)–C(11')	1·4021	1·4032	1·4041
C(10)–C(11)	1·4427	1·4411	1·4399
C(10)–C(12)	1·4347	1·4344	1·4352
C(11)–C(15)	1·4314	1·4296	1·4363
C(12)–C(13)	1·3692	1·3726	1·3744
C(15)–C(14)	1·3640	1·3699	1·3726
C(13)–C(14)	1·4234	1·4251	1·4270
σ_{av} (C–O)	0·0025	0·0013	0·0013
C(4)–O(6)	1·1860	1·1897	1·1919
C(5)–O(8)	1·1973	1·1990	1·2005
C(4)–O(7)	1·4090	1·4082	1·4066
C(5)–O(7)	1·3886	1·3889	1·3884
σ_{av} (C–O)	0·0021	0·0013	0·0013
C(1)–H(1)	0·98	1·00	0·97
C(9)–H(9)	1·03	1·04	1·09
C(12)–H(12)	0·97	0·97	0·90
C(13)–H(13)	0·97	0·98	0·83
C(14)–H(14)	0·99	1·00	0·92
C(15)–H(15)	0·99	0·99	0·93
σ_{av}(C–H)	0·02	0·02	0·06

---

[*] Unless otherwise indicated the XRAY 1976 program library (Stewart, Machin, Dickinson, Ammon, Heck & Flack, 1976) was used for all computerized calculations.

[*] Lists of structure factors and anisotropic thermal parameters have been deposited with the British Library Lending Division as Supplementary Publication No. SUP 33616 (31 pp.). Copies may be obtained through The Executive Secretary, International Union of Crystallography, 5 Abbey Square, Chester CH1 2HU, England.

(REF 2) and (*b*) data consisting only of reflections for which $\sin\theta/\lambda < 0{\cdot}610$ Å^{-1} (REF 3). The last refinement was chosen to be representative of many structure determinations of organic molecules; the resolution is equivalent to a 2θ limit of 140° for Cu *Kα* radiation. The number of contributing data, *R* values and the resulting bond distances with e.s.d.'s are presented in Table 2. The refinement excluding the low-angle data, REF 2, was judged to give the most realistic parameters for the C and O atoms, Table 3. Rigid-body thermal-motion corrections (Schomaker & Trueblood, 1968) were calculated with these parameters, Table 4.

Discussion

The differences in the refined models obtained with the three versions of the data are not great. The e.s.d.'s of the lengths of the C—C and C—O bonds clearly reflect the size of the respective sets of data. Thus they are similar from REF 1 and REF 2 but are approximately twice as large from REF 3. As expected, the e.s.d.'s in the C—H bonds increase markedly when the lower-angle data are excluded.

The smaller differences in the bond distances among the three models refined in this investigation in comparison with those reported for the CN groups in 1,1,2,2-tetracyanocyclopropane are clearly consistent with the concept that the inadequacies of the scattering factors at low $\sin\theta/\lambda$ values increase with increasing bond order. The differences we find are sufficiently small to be within the e.s.d.'s of many structures determined with room-temperature data collected with Cu *Kα* radiation. Nonetheless, the trends are clearly systematic and generally consistent with expectation.

The differences [d(REF 2) − d(REF 3)] are summarized schematically in Fig. 1. In particular the C=O double bonds are lengthened, the neighboring C—C bonds are shortened and the shorter aromatic bonds tend to be lengthened as the effects of valence electrons are excluded from the refinement. The

Table 3. *Positional parameters with e.s.d.'s from REF 2 with* $0{\cdot}478 < \sin\theta/\lambda < 0{\cdot}910$ Å^{-1}

(*a*) Positional parameters of C and O atoms (×10^5)

	x	*y*	*z*
C(1)	−18059 (12)	4860 (8)	−2218 (15)
C(2)	1844 (12)	14136 (8)	5431 (14)
C(3)	19148 (11)	9474 (8)	7627 (14)
C(4)	9056 (14)	29920 (9)	12410 (16)
C(5)	37527 (13)	22390 (9)	16592 (15)
O(6)	−305 (15)	38238 (9)	12605 (18)
O(7)	30691 (12)	34247 (7)	19132 (14)
O(8)	55510 (11)	23494 (9)	21328 (15)
C(9)	−16665 (12)	5478 (8)	47179 (15)
C(10)	3614 (12)	14841 (8)	55465 (13)
C(11)	20682 (12)	9231 (8)	58305 (14)
C(12)	7765 (14)	29848 (8)	60939 (16)
C(13)	27707 (16)	38701 (9)	68698 (16)
C(14)	44633 (15)	33151 (10)	71517 (16)
C(15)	41179 (13)	18855 (10)	66468 (16)

(*b*) Positional and thermal parameters for the H atoms (×10^3). H atoms are assigned the same number as the C atom to which they are bonded.

	x	*y*	*z*	*U* (Å^2)
H(1)	−300 (8)	81 (6)	−35 (10)	44 (9)
H(9)	−306 (10)	87 (7)	430 (12)	55 (11)
H(12)	−33 (7)	330 (5)	598 (8)	36 (7)
H(13)	294 (16)	471 (4)	707 (7)	33 (6)
H(14)	581 (6)	391 (5)	773 (7)	34 (7)
H(15)	514 (7)	146 (5)	678 (8)	37 (7)

Table 4. *Analysis of the thermal parameters of A-PMDA assuming rigid-body motion*

(*a*) Pyromellitic dianhydride

T (Å^2)	0·0117	0·0004	0·0004
		0·0098	0·0012
			0·0109
L (deg^2)	4·2	2·1	0·7
		5·0	0·4
			3·5

S is identically zero.

r.m.s. ΔU_{ij} is 0·0008 Å^2 where ΔU_{ij} is the difference between observed U_{ij} and U_{ij} calculated from rigid-body parameters.

r.m.s. $\sigma(U_{ij})$ is 0·0003 Å^2.

(*b*) Anthracene

T (Å^2)	0·0132	−0·0007	−0·0006
		0·0107	0·0012
			0·0109
L (deg^2)	2·1	2·1	0·2
		5·1	0·3
			0·33

S is identically zero.

r.m.s. ΔU_{ij} is 0·0004 Å^2.

r.m.s. $\sigma(U_{ij})$ is 0·0003 Å^2.

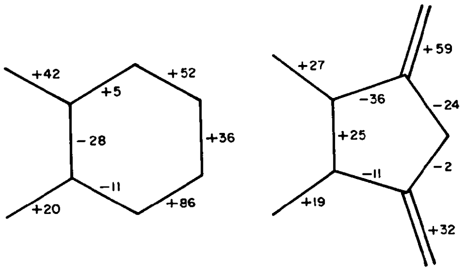

Fig. 1. Changes in bond distances associated with a reduction of the influence of valence electrons on the refinement. The numerical values given are the distances obtained from REF 2 less those obtained from REF 3 (in Å × 10^4).

changes are not the same for chemically equivalent (but crystallographically different) bonds although the differences are not necessarily significant. As will be discussed later, the differences in the changes in the chemically equivalent parts of the anhydride rings are nevertheless consistent with packing effects.

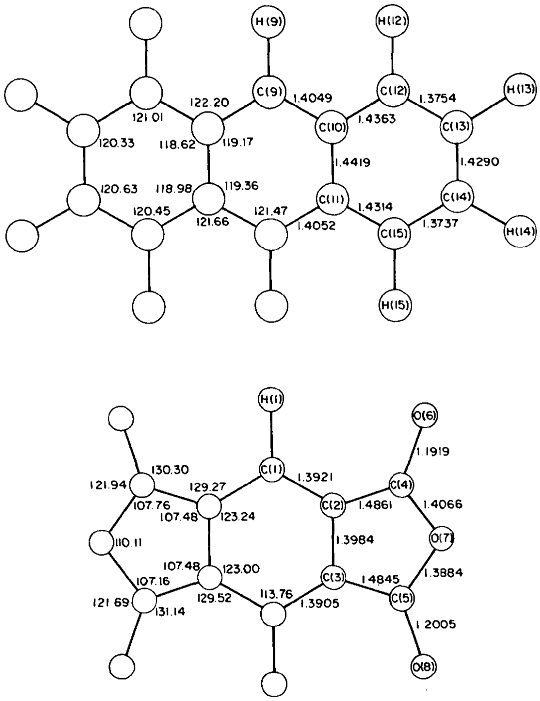

Fig. 2. Atom labeling, bond lengths (Å), and angles (°). The values for anthracene are corrected for thermal effects assuming rigid-body motion. Those for PMDA are not. The e.s.d.'s in the bond angles are *ca* 0·09°. The e.s.d.'s in the bond lengths are similar to those given in Table 2 for REF 2. Neither estimate includes any possible systematic errors introduced by the assumption of rigid-body motion in the case of anthracene.

We have also carried out rigid-body thermal-motion calculations. Pawley & Rinaldi (1972) have shown that a good fit to the observed anisotropic thermal parameters by a rigid body is a necessary but not sufficient condition for establishing that a molecule is rigid. In view of the constraints imposed by the chemical structure of both molecular entities we feel this condition is probably also sufficient for this crystal. We have, however, decided to apply the criterion stringently before accepting the corrections as valid. Both molecules display 0·003 Å^2 average e.s.d.'s in their U_{ij} values. The differences in the values calculated for rigid-body motion and the observed values are 0·0004 Å^2 for anthracene and 0·0008 Å^2 for PMDA. We have therefore decided to accept the corrections for anthracene as valid but not those for PMDA. The bond distances that we will use in further discussion of the structure, those from REF 2 with rigid-body-motion corrections applied to the anthracene molecule but not to PMDA, are presented in Fig. 2.

A stereoscopic packing diagram (Johnson, 1971) is presented in Fig. 3. The crystal may be characterized as consisting of continuous columns, each made up of an identical stack of alternating anthracene and PMDA molecules. They may be visualized as elongated parallelepipeds with their long axis in the [221] direction and stacked in the [001] direction.* Two probable cleavage planes, corresponding to faces of the parallelepiped columns, are apparent in Fig. 3, the most

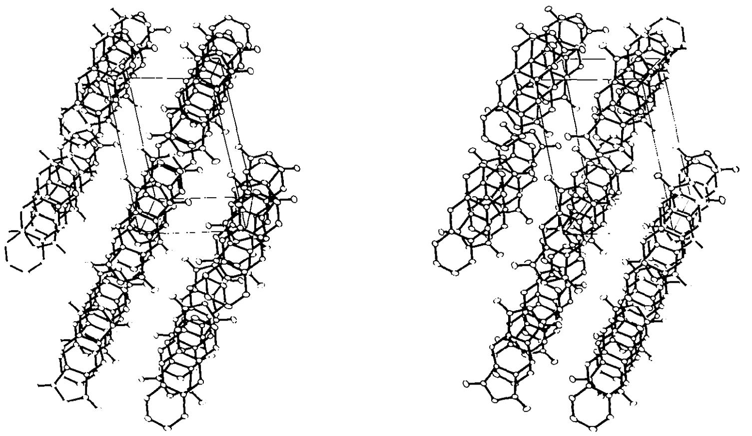

Fig. 3. A stereoscopic representation of the molecular packing viewed normal to the planes of the molecules. The origin is in the back left lower corner. The a axis points to the right and b points up. The c^* axis is therefore out the plane of the page approximately normal to it. H atoms have been omitted for clarity.

---

* When the structure was compared with that reported by Boeyens & Herbstein it was found that their choice of unit cell was different from ours and may be converted to ours by the transformation (101/011/001). The lattice constants thus obtained are a = 7·95, b = 10·75, c = 7·3 Å, α = 116, β = 120, γ = 93°. The convention used here has the advantage that the **c*** vector is approximately normal to the planes of the molecules. The reduced cell may be obtained from that used here by the transformation (001/100/111). The lattice constants thus obtained are a = 7·125, b = 7·281, c = 9·153 Å, α = 69·86, β = 86·86, γ = 68·49°.

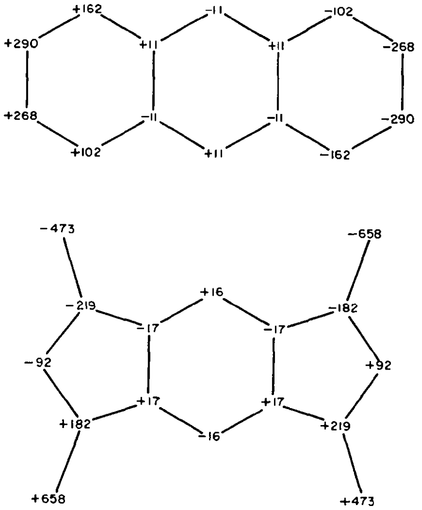

Fig. 4. Distances of atoms from least-squares planes (in Å × 10^4) through the central rings of each molecule.

obvious of which is parallel to the ($1\bar{1}0$) plane and the other of which is parallel to (010).

It is apparent from Fig. 3 that the planes of the anthracene and PMDA molecules are nearly parallel. However, the molecules in adjacent stacks are displaced in the direction normal to the plane by approximately one half the perpendicular intrastack intermolecular distance. This results in an interlocking packing network that is unfavorable for a cleavage plane parallel to the planes of the individual molecules. It is therefore not necessary to invoke charge-transfer forces to explain the fact that the crystals do not readily cleave perpendicular to the stack axis but only along the ($1\bar{1}0$) and (010) planes.

Crystal packing places carbonyl O(6) and O(8) in different environments, Fig. 3. This results in interstack intermolecular interactions which affect the conformation of both the PMDA and anthracene molecules. The relevant contact distances and symmetry operators for the second atom are: [O(6)$\cdots$C(12′) 3·303, O(6)$\cdots$C(13′) 3·478 Å ($1-x$, $-y$, $1-z$)] and [O(8)$\cdots$C(1′) 3·287 Å ($1+x$, y, z)]. All the above contacts are consistent with the observed deviation from planarity, Table 5 and Fig. 4. The anhydride portion of the PMDA molecule is twisted as the result of the different directions from which these contacts originate, while the anthracene molecule is slightly folded about C(10)–C(11). For the latter molecule, the short interstack contacts occur on only one side of the symmetry-independent end ring.

Table 5. *Least-squares planes and lines*

The x, y and z axes of the orthogonal coordinate system are in the directions $\mathbf{a}$, $\mathbf{b}^*$ and $\mathbf{a} \times \mathbf{b}^*$ respectively. In that coordinate system:

The plane of the central ring of pyromellitic dianhydride is given by

$$-0{\cdot}2019x + 0{\cdot}3149y + 0{\cdot}9274z = 0{\cdot}0.$$

The plane of the central ring of anthracene is given by

$$-0{\cdot}2449x + 0{\cdot}3377y + 0{\cdot}9089z = 3{\cdot}3320.$$

The line of the long axis of pyromellitic dianhydride is given by

$$\begin{aligned} x &= 0{\cdot}0000 + 0{\cdot}3706t \\ y &= 0{\cdot}0000 + 0{\cdot}9015t \\ z &= -0{\cdot}0000 - 0{\cdot}2234t. \end{aligned}$$

The line of the long axis of anthracene is given by

$$\begin{aligned} x &= -1{\cdot}3063 + 0{\cdot}4382t \\ y &= 0{\cdot}0000 + 0{\cdot}8732t \\ z &= 3{\cdot}3141 - 0{\cdot}2134t. \end{aligned}$$

In terms of $\mathbf{a}$, $\mathbf{b}$ and $\mathbf{c}$ and in terms of the unit vectors of the orthogonal coordinate system, $\hat{\mathbf{i}}$, $\hat{\mathbf{j}}$ and $\hat{\mathbf{k}}$, the unit normal of the central ring of the pyromellitic dianhydride molecule may be expressed as:

$$\begin{aligned} \mathbf{N}(\text{PMDA}) &= 0{\cdot}0405\mathbf{a} + 0{\cdot}0354\mathbf{b} + 0{\cdot}1714\mathbf{c} \\ \text{and } \mathbf{N}(\text{PMDA}) &= -0{\cdot}2019\hat{\mathbf{i}} + 0{\cdot}3149\hat{\mathbf{j}} + 0{\cdot}9274\hat{\mathbf{k}}. \end{aligned}$$

The normal to the central plane of the anthracene molecule may be expressed as:

$$\begin{aligned} \mathbf{N}(\text{A}) &= 0{\cdot}0349\mathbf{a} + 0{\cdot}0380\mathbf{b} + 0{\cdot}1709\mathbf{c} \\ \text{and } \mathbf{N}(\text{A}) &= -0{\cdot}2449\hat{\mathbf{i}} + 0{\cdot}3377\hat{\mathbf{j}} + 0{\cdot}9089\hat{\mathbf{k}}. \end{aligned}$$

The angle between this normal and the $\mathbf{c}$ axis is 20·7°.

The angle between the long axes of anthracene and pyromellitic dianhydride is 4·2°.

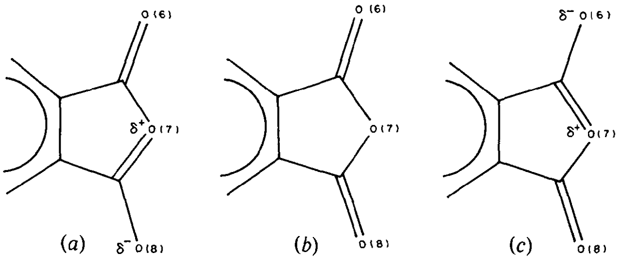

Fig. 5. Canonical forms contributing to the equilibrium of the PMDA moiety.

The differences in environments of the two carbonyl groups also appear to give rise to the observed variations in the bond distances in the formally chemically equivalent C=O bonds of the symmetry-independent anhydride moiety. The differences appear to stem from an electronic rather than a steric effect; *i.e.*, from a disturbance of the equilibrium depicted schematically in Fig. 5. The canonical forms participating in the equilibrium are analogous to those described by Merlino (1971) for esters and lactones. In a symmetrical environment, the population of canonical forms 5(*a*) and 5(*c*) would be identical and the appropriate C–O distances would be equal. In this structure, crystal packing places two symmetry-related O(6) atoms in closer contact than two symmetry-related O(8) atoms, 3·725 and 4·294 Å, respectively. Canonical forms 5(*a*) and 5(*c*) have localized negative charges on O(8) and O(6), respectively. Thus, in the crystalline environment, the repulsive force, which varies with $1/r^2$, between symmetry-related O(6) atoms would be larger than between O(8) atoms $[r^2\mathrm{O}(6)/r^2\mathrm{O}(8) = 0{\cdot}75]$. Therefore, canonical form 5(*a*) would be expected to make a greater contribution to the resonance structure than 5(*c*). Further substantiation of this mechanism is provided by the changes observed in the bond distances when the lower-angle data are removed. The changes in the anhydride moiety were greater in each bond involving the carbonyl group at C(4). This may be taken as evidence that there is greater π-electron density in the C(4)–O(6) than in the C(5)–O(8) bond. While this mechanism is fully consistent with the observations, it must be emphasized that much of the evidence to support it comes from differences in bond distances that are not much greater than their e.s.d.'s. Clearly, further high-resolution structural studies are needed before one can consider the mechanism to be established.

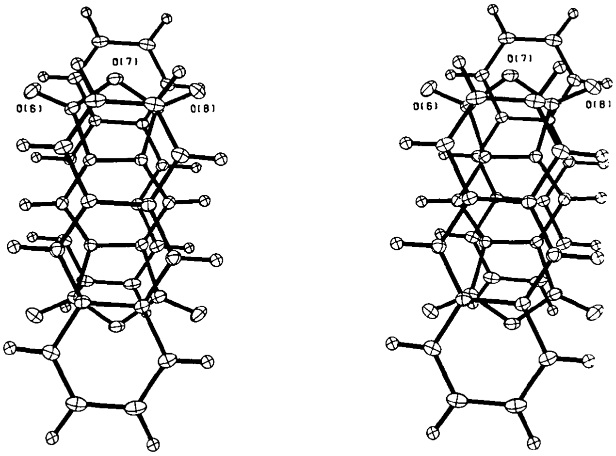

Fig. 6. Overlap of an acceptor molecule with the donor molecules above and below it.

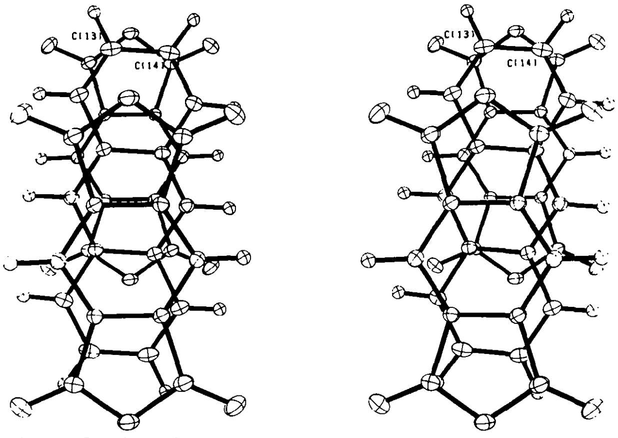

Fig. 7. Overlap of a donor molecule with the acceptor molecules above and below it.

With the above points in mind, concerning the accuracy of the bond lengths we report, the observations that the distortions of the molecule from planarity are traceable to packing effects and that the differences in the C–O bond distances of the anhydride moiety are also reasonably traceable to an electronic aspect of packing interactions, we now turn to the intrastack interactions. Fig. 3 shows that the molecules pack so that the central benzene rings are in a staggered relationship; *i.e.*, the bonds common to two rings are near the center of five- or six-membered rings of the adjacent molecules within a stack. Further details of the overlap of adjacent molecules are given in Figs. 6 and 7. The interplanar angle between the least-squares mean planes fit to the respective central benzene rings, Table 5, is 3·0° and the angle between the least-squares lines fit to the long axis of each molecule is 4·2°.

The intrastack intermolecular contact distances between a symmetry-independent anhydride moiety and the anthracene molecules above and below it are significantly different, Fig. 6. We will describe the intrastack environment of the anhydride ring with the labelled O atoms and will refer to the anthracene molecule above it as molecule *A* and that below it as $A\bar{c}$ (where $\bar{c}$ = symmetry operator $x, y, z-1$). Since each molecule lies on a crystallographic inversion center, the description applies *via* an inversion operator to the other anhydride ring of the same molecule. Molecule *A* is in significantly closer contact with the anhydride ring and C(1) and C(3) than is molecule $A\bar{c}$. The relevant contact distances with *A* are: [C(9)···C(3′)] = 3·387, [C(10)···C(1)] = 3·355, [C(12)···C(2)] = 3·327, [C(13)···C(4)] = 3·315, and [C(14)···C(5)] = 3·331 Å. The shortest contact distance for molecule $A\bar{c}$ is [O(8)···C(15′)] = 3·418 Å and for a C–C contact is [C(4)···C(10′)] = 3·438 Å. Thus one can describe the interaction between PMDA and anthracene as being stronger above the plane of the acceptor molecule for one anhydride ring and stronger below it for the other. Similarly, for the anthracene, Fig. 7, one end of the donor has a stronger interaction with the acceptor above the plane of the molecule while the other end has the same interaction below this plane.

Several crystal structure determinations have been reported for anthracene. We believe that the neutron diffraction study of perdeuteroanthracene (Lehmann & Pawley, 1972) presents the most accurate bond distances and will therefore use it for a comparison with anthracene in this complex. Bond lengths, corrected for thermal motion and averaged according to *mmm* symmetry, for uncomplexed perdeuteroanthracene and for the anthracene of this investigation are presented in Table 6. The e.s.d.'s for the former are the literature values and for the latter are 1·5 times those from the full-matrix least-squares refinement; the multiplier was used to allow for some additional uncertainty in the thermal-motion corrections. Two comments for the

Table 6. *Comparison of bond lengths of anthracene in perdeuteroanthracene and A-PMDA* (Å)

	Perdeuteroanthracene	A-PMDA
C(9)–C(10), C(9)–C(11)	1·402 (2)	1·405 (2)
C(10)–C(11)	1·439 (3)	1·442 (2)
C(10)–C(12), C(11′)–C(15)	1·433 (2)	1·434 (2)
C(12)–C(13), C(15)–C(14)	1·368 (2)	1·375 (2)
C(13)–C(14)	1·432 (3)	1·429 (2)

Table 7. *Comparison of bond lengths of pyromellitic dianhydride in A-PMDA, P-PMDA and PMDA* (Å)

	A-PMDA	P-PMDA*	PMDA†
C(1)–C(2), C(1)–C(3′)	1·391	1·381	1·383
C(2)–C(3)	1·398	1·379	1·389
C(2)–C(4), C(3)–C(5)	1·485	1·474	1·485
C(4)–O(6), C(5)–O(8)	1·196	1·196	1·187
C(4)–O(7), C(5)–O(7)	1·398	1·382	1·388

* Evans & Robinson (1977).
† Irngartinger (1977).

tabulated values are appropriate: (*a*) The maximum deviation from the average values within this investigation is 0·0025 Å, (*b*) the bond distances for anthracene in the complex and in the uncomplexed form are remarkably similar.

A crystal structure analysis has recently been carried out for uncomplexed PMDA (Irngartinger, 1977) and for a phenanthrene–PMDA complex, P-PMDA (Evans & Robinson, 1977). Bond distances, averaged to reflect *mmm* symmetry, from these two structures are presented in Table 7. The tabulated bond distances for PMDA deviate no more than 0·010 Å from those we report for A-PMDA and those for the acceptor in P-PMDA differ by no more than 0·019 Å. In both cited structures, the bond distances are generally shorter than the values we have determined. These differences are more likely traceable to thermal motion in the room-temperature structures and to valence-electron effects than to any effects resulting from charge transfer.

In view of the demonstrated similarities between complexed anthracene and pyromellitic dianhydride in this investigation and their respective uncomplexed parent compounds in independent investigations, we conclude that even high-resolution, low-temperature crystal structure analysis has not revealed any clearly significant changes in bond distances attributable to charge-transfer interaction.

The authors thank the Alexander von Humboldt Foundation of West Germany and the National Research Council of Canada for the award of a Humboldt Fellowship and a Travel Fellowship to B. E. Robertson, the Institut für Organische Chemie, Biochemie und Isotopenforschung der Universität Stuttgart for assistance and C. Eckhardt, Department of Chemistry, University of Nebraska, and N. Karl, Physikalisches Institut, Teil 3 und Kristallabor der Universität Stuttgart, for samples and helpful discussions.

References

Boeyens, J. C. A. & Herbstein, F. H. (1965). *J. Phys. Chem.* **69**, 2160–2176.

Eckhardt, C. J. & Merski, J. (1973). *Surf. Sci.* **37**, 937–946.

Evans, D. L. & Robinson, W. T. (1977). *Acta Cryst.* B**33**, 2891–2893.

Haarer, D. & Karl, N. (1973). *Chem. Phys. Lett.* **21**, 49–53.

Irngartinger, H. (1977). Private communication.

Johnson, C. K. (1971). *ORTEP*-II. Report ORNL-5138. Oak Ridge National Laboratory, Tennessee.

Karl, N. & Ziegler, J. (1975). *Chem. Phys. Lett.* **32**, 438–442.

Keijzers, C. P. & Haarer, D. (1977). *J. Chem. Phys.* **67**, 925–932.

Lehmann, M. S. & Pawley, G. S. (1972). *Acta Chem. Scand.* **26**, 1996–2004.

Lemley, J. T., Skarstad, P. M. & Hughes, R. E. (1976). *Acta Cryst.* B**32**, 35–40.

Merlino, S. (1971). *Acta Cryst.* B**27**, 2491–2492.

Pawley, G. S. & Rinaldi, R. P. (1972). *Acta Cryst.* B**28**, 3605–3609.

Schomaker, V. & Trueblood, K. N. (1968). *Acta Cryst.* B**24**, 63–76.

Stewart, J. M., Machin, P. A., Dickinson, C., Ammon, H. L., Heck, H. & Flack, H. (1976). The XRAY 76 system. Tech. Rep. TR-446. Computer Science Center, Univ. of Maryland, College Park, Maryland.

Ziegler, J. & Karl, N. (1978). To be published.